© 2019. Published by The Company of Biologists Ltd | Journal of Cell Science (2019) 132, jcs226019. doi:10.1242/jcs.226019

RESEARCH ARTICLE

# STIM1 phosphorylation at $Y^{316}$ modulates its interaction with SARAF and the activation of SOCE and $I_{CRAC}$

**Esther Lopez[1,*], Irene Frischauf[2], Isaac Jardin[1], Isabella Derler[2], Martin Muik[2], Carlos Cantonero[1], Gines M. Salido[1], Tarik Smani[3], Juan A. Rosado[1,‡] and Pedro C. Redondo[1,‡,§]**

## ABSTRACT

Stromal interaction molecule 1 (STIM1) is one of the key elements for the activation of store-operated $Ca^{2+}$ entry (SOCE). Hence, identification of the relevant phosphorylatable STIM1 residues with a possible role in the regulation of STIM1 function and SOCE is of interest. By performing a computational analysis, we identified that the $Y^{316}$ residue is susceptible to phosphorylation. Expression of the STIM1-Y316F mutant in HEK293, NG115-401L and MEG-01 cells resulted in a reduction in STIM1 tyrosine phosphorylation, SOCE and the $Ca^{2+}$ release-activated $Ca^{2+}$ current ($I_{CRAC}$). STIM1–Orai1 colocalization was reduced in HEK293 cells transfected with YFP–STIM1-Y316F compared to in cells with wild-type (WT) YFP-tagged STIM1. Additionally, the Y316F mutation altered the pattern of interaction between STIM1 and SARAF under resting conditions and upon $Ca^{2+}$ store depletion. Expression of the STIM1 Y316F mutant enhanced slow $Ca^{2+}$-dependent inactivation (SCDI) as compared to STIM1 WT, an effect that was abolished by SARAF knockdown. Finally, in NG115-401L cells transfected with shRNA targeting SARAF, expression of STIM1 Y316F induced greater SOCE than STIM1 WT. Taken together, our results provide evidence supporting the idea that phosphorylation of STIM1 at $Y^{316}$ plays a relevant functional role in the activation and modulation of SOCE.

**KEY WORDS: Tyrosine phosphorylation, STIM1, Orai1, $Y^{316}$, $I_{CRAC}$, SARAF**

## INTRODUCTION

Store-operated $Ca^{2+}$ entry (SOCE) participates in the intracellular $Ca^{2+}$ homeostasis of both excitable and non-excitable cells. Physiological agonists evoke the depletion of intracellular $Ca^{2+}$ reservoirs leading to an interaction between the endoplasmic reticulum (ER) $Ca^{2+}$ sensor, STIM1 and Orai1, the $Ca^{2+}$-permeable channel located at ER–plasma membrane (PM) junctions, thus allowing $Ca^{2+}$ entry. STIM1 contains an ER luminal N-terminal portion that includes a canonical EF-hand (amino acids 63–98) responsible for the $Ca^{2+}$ binding, and further, a sterile alpha motif (SAM; amino acids 131–200) that contributes to STIM1 multimerization. After this motif, STIM1 contains its single transmembrane domain, and then, the cytosolic STIM1 region, which exhibits three coiled-coil domains (CC1, CC2 and CC3) the latter two of which contain the STIM1–Orai1-activating region (SOAR). Additionally, an auto-inhibitory region, including an acidic domain ($E^{318}$–$E^{322}$) located in the CC1 region and a polybasic domain ($K^{382}$–$K^{387}$) in the CC2 can be found, which occlude the SOAR maintaining STIM1 in a quiescent state (Fahrner et al., 2014; Korzeniowski et al., 2010; Yuan et al., 2009; Zhou et al., 2013). Finally, the C-terminal domain of STIM1 exhibits the STIM1 C-terminal inhibitory domain (CTID; amino acids 448–530), which is responsible for the interaction with the $Ca^{2+}$ entry regulatory protein SOCE-associated regulatory factor (SARAF), which regulates the slow $Ca^{2+}$-dependent inactivation of Orai1 (SCDI) (Derler et al., 2016; Haniu et al., 2006; Perni et al., 2015). Structural and molecular analyses have revealed that in order to regulate the STIM1–Orai1 interaction, SARAF interacts with the CTID downstream of the SOAR region (Jha et al., 2013). CTID consists of two lobes (STIM1 448–490 and STIM1 490–530). The STIM1 (490–530) lobe directs SARAF to the SOAR; meanwhile the STIM1 (448–490) lobe wraps around the SOAR to restrict access of SARAF to the SOAR (Jha et al., 2013).

Recent studies have reported that STIM1 remains in a tightly packed conformation in resting cells (Ma et al., 2015; Muik et al., 2011). According to this hypothesis, after intracellular $Ca^{2+}$ store depletion, STIM1 undergoes a conformational change resulting in the full extended and active configuration, thus, accommodating the C-terminal region of Orai1. The CC1 inhibitory domain of STIM1 has been reported to maintain STIM1 in a quiescent state by hiding the SOAR domain in non-stimulated cells (Haniu et al., 2006; Jha et al., 2013; Palty et al., 2012). In addition, recent studies have demonstrated that $Ca^{2+}$-mediated dissociation of the STIM1 EF-hand domain during store depletion triggers the rearrangement of STIM1 EF-hand, SAM and transmembrane domains, which allows the reorganization of the cytosolic portion of STIM1, and subsequently, releases SOAR from the CC1 domain in order to interact with and activate Orai1 (Ma et al., 2015).

STIM1 phosphorylation has been reported to play a relevant role during its function. Phosphorylation of STIM1 at $S^{486}$ and $S^{668}$ has been shown to lead to SOCE suppression during mitosis (Smyth et al., 2009). Furthermore, STIM1 has been reported to be a target of ERK1 and ERK2 (ERK1/2, also known as MAPK3 and MAPK1, respectively), which phosphorylate STIM1 at $S^{575}$, $S^{608}$ and $S^{621}$ upon $Ca^{2+}$ store depletion; this leads to the dissociation from the microtubule plus-end-binding protein EB1 and the activation of Orai1 and SOCE (Pozo-Guisado et al., 2010, 2013). Phosphorylation of STIM1 at $S^{575}$ by ERK1/2 is essential for myoblast differentiation (Lee et al., 2012) and is inhibited by 17β-estradiol in airway epithelia, thus reducing SOCE and increasing the risk of lung diseases (Sheridan et al., 2013).

[1]Department of Physiology, Cell Physiology Research Group, Institute of Molecular Pathology Biomarkers, University of Extremadura, 10003 Caceres, Spain. [2]Molecular & Membrane Biophysics, Institute of Biophysics, Johannes Kepler University Linz, A-4020 Linz, Austria. [3]Department of Medical Physiology and Biophysics, Institute of Biomedicine of Seville (IBiS)/University of Seville/CIBERCV, 41013 Seville, Spain.
*Present address: Stem Cell Therapy Unit, Jesús Usón Minimally Invasive Surgery Centre, 10071 Cáceres, Spain
‡These authors contributed equally to this work

§Author for correspondence (pcr@unex.es)

P.C.R., 0000-0002-2067-2627

**Received 1 October 2018; Accepted 8 April 2019**

Journal of Cell Science (2019) 132, jcs226019. doi:10.1242/jcs.226019

Moreover, EGF-stimulated phosphorylation of STIM1 at $S^{575}$, $S^{608}$ and $S^{621}$ is required for human endometrial adenocarcinoma cell migration (Casas-Rua et al., 2015). In addition, phosphorylation of STIM1 at $T^{389}$ by protein kinase A (PKA) induces selective activation of acid-regulated $Ca^{2+}$-selective (ARC) channels while reducing the ability of STIM1 to activate $Ca^{2+}$ release-activated $Ca^{2+}$ current (CRAC) channels (Thompson and Shuttleworth, 2015). The role of tyrosine phosphorylation in STIM1 function has been scarcely investigated. Tyrosine kinase activation by intracellular $Ca^{2+}$ store depletion, and subsequent activation of $Ca^{2+}$ entry, has previously been reported (Mills et al., 2015; Sage et al., 1992; Zuo et al., 2011). Interestingly, $Ca^{2+}$ store depletion by thapsigargin (TG) has been reported to evoke protein tyrosine phosphorylation in cells loaded with the $Ca^{2+}$ chelator BAPTA (Sargeant et al., 1994), indicating that $Ca^{2+}$ store depletion itself, and not the subsequent rise in the cytosolic free $Ca^{2+}$ concentration ($[Ca^{2+}]_c$), is sufficient for tyrosine kinase activation. We have previously reported that, in BAPTA-loaded cells, STIM1 is phosphorylated at tyrosine residues upon $Ca^{2+}$ store depletion, an event that is relevant for STIM1–Orai1 interaction (López et al., 2012). Btk activation and subsequent regulation of SOCE in human platelets and murine B cells have been described (Fluckiger et al., 1998; Redondo et al., 2005), and we have reported interaction between Btk and STIM1 as well as Btk-dependent tyrosine phosphorylation of STIM1 in human platelets (López et al., 2012). In addition, a recent study has revealed that phosphorylation of STIM1 at $Y^{361}$ is important for the recruitment of Orai1 into STIM1 puncta and the activation of SOCE (Yazbeck et al., 2017). Furthermore, the $Y^{316}$ residue has been found to play a relevant role in maintaining STIM1 in a quiescent state in resting cells (Yu et al., 2013). Here, we show that phosphorylation of STIM1 at $Y^{316}$ plays an essential role in the STIM1 and Orai1 colocalization at ER–PM junctions, as well as for the activation of $I_{CRAC}$ and SOCE. We also describe for the first time that phosphorylation of STIM1 at $Y^{316}$ modulates the interaction between STIM1 and its regulator SARAF, hence, regulating SCDI. Taken together, these findings might shed new light on the molecular mechanism of SOCE activation and modulation.

## RESULTS

### Identification of phosphorylation of tyrosine residues in STIM1 upon $Ca^{2+}$ store depletion

Computational analysis using the NetPhos 2.0 Server revealed six alignment sequences that are susceptible to phosphorylation (http://www.cbs.dtu.dk/services/NetPhos/). Among them, the score of three sequences (leading to phosphorylation of $Y^{231}$, $Y^{316}$ and $Y^{361}$) was sufficiently high for them to be considered as targets of tyrosine kinases; however, only two of them are present in the cytosolic region of STIM1, $Y^{316}$ and $Y^{361}$, which are located in the CC1 and CC2 (SOAR) domains, respectively (Table 1). $Y^{361}$ phosphorylation was recently described as a relevant posttranslational modification required for Orai1–STIM1 interaction during SOCE in human pulmonary arterial endothelial (HPAE) cells (Yazbeck et al., 2017). In these cells, STIM1 phosphorylation at $Y^{316}$ was found to have a minor effect on SOCE. However, these findings disagree with a previous study where the authors proposed a relevant role for STIM1 $Y^{316}$ phosphorylation in the maintenance of STIM1 in a closed conformation in quiescent cells (Yu et al., 2013). Taking into account this controversy, we explored the role of $Ca^{2+}$ store depletion in the phosphorylation of both residues ($Y^{316}$ and $Y^{361}$) in HEK293 cells expressing either wild-type (STIM1 WT) or STIM1 mutants where we replaced the target tyrosine residues with phenylalanine, another aromatic amino acid that avoids the alteration of the structure of the STIM1 auto-inhibitory domain (Yu et al., 2013). As depicted in the Fig. 1A, treatment of HEK293 cells expressing STIM1 WT with TG evoked an increase in STIM1 tyrosine phosphorylation, as previously described in platelets (López et al., 2012). Overexpression of STIM1 Y316F impaired TG-evoked STIM1 phosphorylation (Fig. 1A,C; $n$=4). We have also found a significant reduction in TG-induced STIM1 tyrosine phosphorylation in HEK293 expressing the STIM1 Y361F mutant, as previously described in HPAE cells (Yazbeck et al., 2017). STIM1 tyrosine phosphorylation induced by TG was reduced to 39.3±9.0% (mean±s.e.m.) in HEK293 cells expressing STIM1 Y316F compared to cells expressing STIM1 WT, while less inhibition was observed in cells transfected with Y361F (Fig. 1A,C; $n$=3–5; $P$<0.05).

To confirm these results, we analyzed STIM1 phosphorylation at $Y^{316}$ and $Y^{361}$ in the STIM1-deficient NG115-401L cell line (Albarran et al., 2016; Zhang et al., 2015; Zhang and Thomas, 2016). Expression of the STIM1 Y316F mutant in NG115-401L cells attenuated the STIM1 phosphotyrosine content at resting conditions and upon stimulation with TG as compared with those cells expressing STIM1 WT (Fig. 1B,C; $n$=5). In addition, our results indicate that mutation of the tyrosine residue to a phenylalanine residue is an efficient mechanism to analyze STIM1 phosphorylation during SOCE, since this change might avoid the constitutive activation of STIM1 observed when $Y^{316}$ is replaced by an alanine or aspartate residue as previously demonstrated (Yu et al., 2013). Similarly, a reduction in the STIM1 phosphotyrosine level was observed in cells expressing YFP–STIM1-Y361F.

### Relevance of $Y^{316}$ in the activation of SOCE

A previous study has reported that phosphorylation of STIM1 at $Y^{316}$ plays a relevant role in maintaining STIM1 in an inactive state in quiescent cells (Yu et al., 2013). Hence, we have further explored the role of the $Y^{316}$ and $Y^{361}$ residues in the STIM1 function during the activation of SOCE. Expression of STIM1 WT restored TG-evoked $Ca^{2+}$ entry in NG115-401L cells as previously reported (Albarran et al., 2016). As shown in Fig. 2A, we observed an

**Table 1. The cytosolic domain of STIM1, highlighting the possible tyrosine phosphorylation sites as predicted by using the NetPhos 2.0 Server from the Technical University of Denmark**

| | Pos | Context | Score | Predication | Functional domain |
|---|---|---|---|---|---|
| Sequence | 231 | CWFA**Y**IQNR | 0.653 | | Transmembrane-domain |
| Sequence | 236 | IQNR**Y**SKEH | 0.028 | | non-described |
| Sequence | 316 | SRQK**Y**AEEE | 0.753 | **$** | CC1: α3 inhibitory domain |
| Sequence | 342 | HSSW**Y**APEA | 0.125 | | CC1: α3 inhibitory domain |
| Sequence | 361 | VEVQ**Y**YNIK | 0.887 | **$** | CC2: α3 inhibitory domain (SOAR) |
| Sequence | 362 | EVQY**Y**NIKK | 0.160 | | CC2: α3 inhibitory domain (SOAR) |

Result of the informatics analysis using the NetPhos 2.0 server for predicting possible tyrosine phosphorylation residues within the STIM1 structure. **$**: indicates the Y residues that reached the maximum scores.

Journal of Cell Science (2019) 132, jcs226019. doi:10.1242/jcs.226019

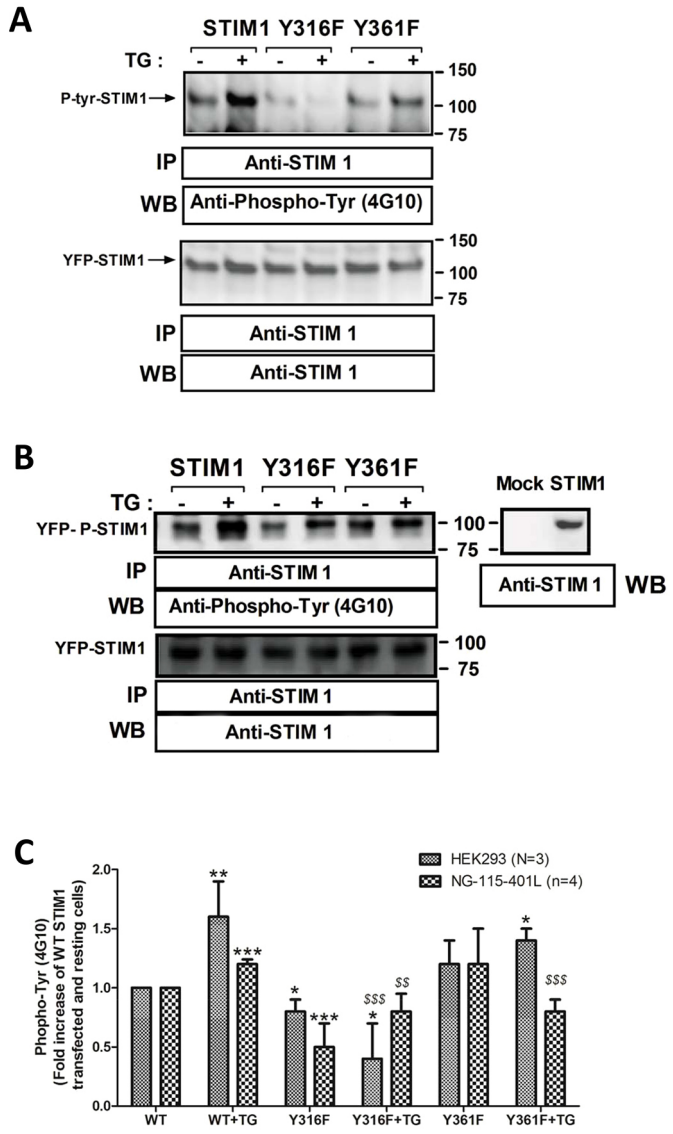


**Fig. 1. Mutation of the tyrosine residues within the STIM1 structure impairs STIM1 tyrosine phosphorylation.** HEK293 cells (A) and NG115-401L cells (B) were transfected with YFP–STIM1-WT or YFP–STIM1 mutant (Y316F or Y361F) overexpression plasmid. Cells were stimulated for 2.5 s with TG (200 nM) in a $Ca^{2+}$-free medium (EGTA, 75 µM was added) and then lysed. Whole-cell lysates were immunoprecipitated (IP) with an anti-STIM1 antibody and immunoprecipitates were subjected to SDS-PAGE (10% gels). Subsequent western blotting (WB) was performed using an anti-phosphotyrosine (4G10) antibody as described in the Materials and Methods. Membranes were re-probed with anti-STIM1 antibody as a protein loading control and to confirm the exogenous expression of STIM1 in NG115-401L cells [mock (empty vector) cells on the right-hand side]. Images are representative of four to six independent experiments. (C) Bar graph represents the mean±s.e.m. of the fold change of the STIM1 phosphotyrosine level as compared to the cells expressing the YFP–STIM1-WT plasmid (level set at 1). *$P$<0.05, **$P$<0.01, ***$P$<0.001 with respect to resting cells expressing YFP–STIM1-WT; $^{\$}P$<0.05, $^{\$\$}P$<0.01, $^{\$\$\$}P$<0.001 with respect to cells expressing YFP– STIM1-WT and stimulated with TG (ANOVA, Dunnett's test).

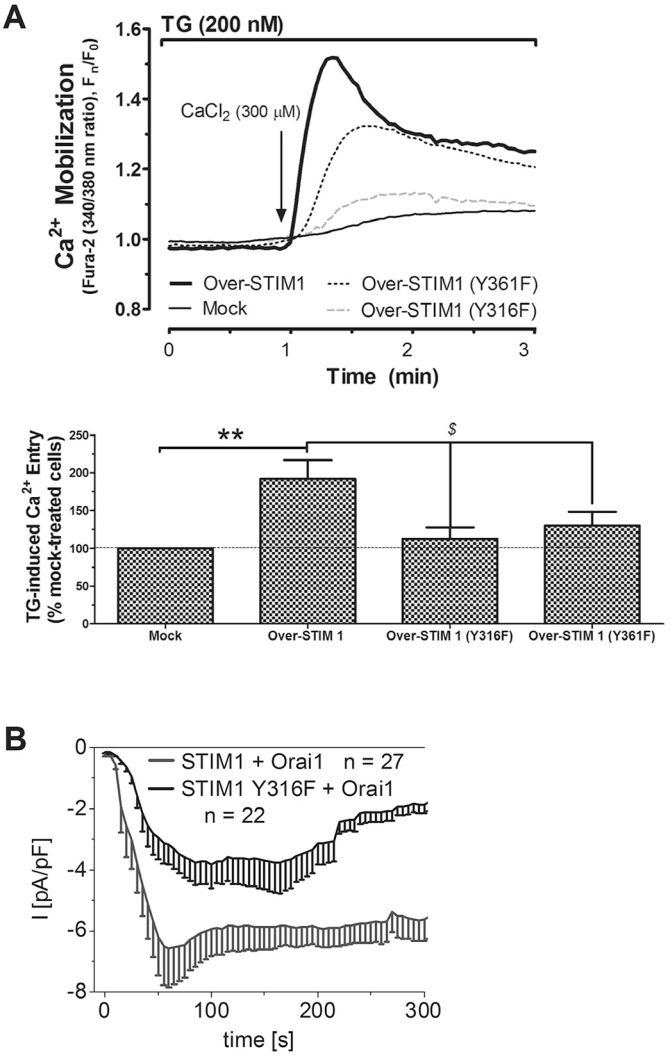


**Fig. 2. STIM1 tyrosine phosphorylation is crucial for TG-evoked SOCE and $I_{CRAC}$ activation.** (A) NG115-401L cells were transfected with YFP–STIM1-WT, the indicated YFP–STIM1 mutants (i.e. overexpression, denoted by over) or the empty vector (Mock). Cells were perfused with a $Ca^{2+}$-free medium (EGTA, 75 µM was added) and then pre-stimulated with TG (200 nM). To detect the SOCE, $CaCl_2$ (300 µM) was added to the extracellular medium. Traces are representative of six independent experiments including 30–40 cells each. The bar graph represents the differences in the TG-induced $Ca^{2+}$ entry, estimated as described in the Materials and Methods section (mean±s.e.m.). **$P$<0.01 compared to mock-treated cells; $^{\$}P$<0.05 compared to cells expressing YFP–STIM1-WT (ANOVA, Dunnett's test). (B) HEK293 cells were simultaneously co-transfected with Orai1 and either STIM1 WT or STIM1 Y316F. The time course of inward currents from whole-cell patch-clamp experiments co-expressing Orai1 with STIM1 WT (gray trace) or STIM1 Y316F (black trace) is shown. Data are presented as the mean±s.e.m. of 22 and 27 cells, as indicated.

increase in TG-evoked SOCE of 91±24% (mean±s.e.m.) in the area under the curves for cells expressing YFP–STIM1 compared to cells expressing the empty vector (mock cells) (Fig. 2A; $P$<0.01, $n$=6). The analysis of the rate of increase in $[Ca^{2+}]_c$ evoked by TG, revealed a $K_1$ of $3.6\times10^{-5}\pm1.5\times10^{-6}$ in mock cells and of $7.6\times10^{-5}\pm1.9\times10^{-6}$ in YFP–STIM-WT cells. YFP–STIM1-WT expression also enhanced SOCE by 47±26% in MEG-01 cells (see Fig. S1; $n$=4–6; $P$<0.001). Interestingly, expression of the STIM1 Y316F mutant significantly reduced SOCE both in NG115-401L and MEG-01 cells (Fig. 2A and Fig. S1, respectively; $P$<0.001; $n$=8). NG115-401L cells expressing YFP–STIM1-Y316F presented a reduction in the area under the curves of 79% with respect to cells expressing the YFP–STIM1-WT, resulting in similar values to those found in mock cells, and subsequently the observed $K_1$ was also similar to that found in mock cells ($3.8\times10^{-6}\pm1.1\times10^{-6}$). As previously reported (Yazbeck et al., 2017),

Journal of Cell Science (2019) 132, jcs226019. doi:10.1242/jcs.226019

we found that expression of STIM1 Y361F attenuated TG-evoked SOCE in NG115-401L cells (Fig. 2A), which confirms that phosphorylation of STIM1 at $Y^{361}$ plays an important role in SOCE.

According to the inhibitory role evidenced by the Y316F or Y361F mutations of STIM1, we consider that Y316F might be more relevant for STIM1 function in the cell models investigated, and hence should be studied further. To this end, we further evaluated whether $Y^{316}$ phosphorylation is relevant for the activation of $I_{CRAC}$ by employing the patch-clamp technique in the whole-cell configuration. HEK293 cells were co-transfected with YFP–STIM1-WT or YFP–STIM1-Y316F, and CFP–Orai1, and we measured the inward currents upon passive store-depletion evoked by employing 20 mM EGTA in the pipette solution (following whole-cell formation) in response to repetitive voltage-ramps from −90 mV to +90 mV applied from a holding potential of 0 mV. Current values were taken from each trace at −74 mV to generate the time-course depicted in Fig. 2B. Store-operated activation of HEK293 cells transfected with YFP–STIM1-WT and CFP–Orai1 reached a maximal inward current at ∼50 s (Fig. 2B, gray trace). By contrast, HEK293 cells containing YFP–STIM1-Y316F displayed a ∼50 s delayed activation to maximal current levels and significantly reduced current density (Fig. 2B, black trace).

### Role of STIM1 $Y^{316}$ phosphorylation in the interaction between STIM1 and Orai1

Orai1 opening is driven by its interaction with STIM1 at ER–PM junctions (Lee et al., 2010). Because phosphorylation of STIM1 at $Y^{316}$ plays an important role in SOCE and $I_{CRAC}$, we analyzed whether this event is relevant for the interaction between STIM1 and Orai1 by looking for colocalization between STIM1 and Orai1 in HEK293 cells co-transfected with YFP–STIM1-WT or STIM1 mutants, and CFP–Orai1. As shown in Fig. 3A, a significant increase in the colocalization between STIM1 and Orai1 is observed upon stimulation with TG (see Fig. 3A.1). Interestingly, expression of the STIM1 Y316F mutant significantly attenuated TG-induced STIM1–Orai1 colocalization (Fig. 3A.2 and bar graph). We found that TG was able to induce colocalization of STIM1 and the Orai1 R91W mutant, which has been reported to be unable to induce $Ca^{2+}$ entry (Liao et al., 2008), thus suggesting that the effect observed with the Y316F mutant reveals a specific role of $Y^{316}$ phosphorylation and is not due to other non-specific effects (Fig. 3A.3).

Co-immunoprecipitation was performed in NG115-401L cells expressing GFP–Orai1 and YFP–STIM1 to prevent changes in the Orai1:STIM1 stoichiometry (Hoda et al., 2006). As shown in the left two lanes of Fig. 3B, Orai1 was detected in STIM1

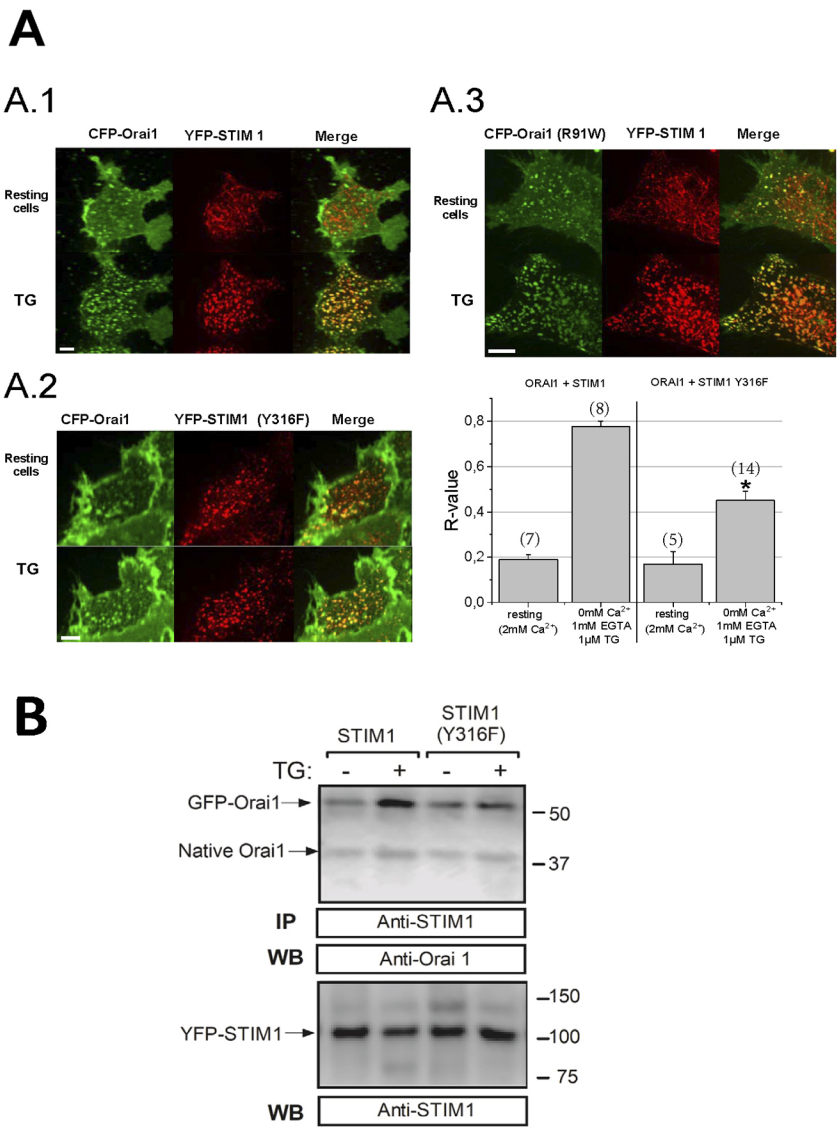


**Fig. 3. STIM1 $Y^{316}$ is required for Orai1 and STIM1 interaction and cell colocalization.** (A) HEK293 cells were transfected with YFP–STIM1-WT (A.1 and A.3) or YFP–STIM1-Y316F (A.2), and with CFP–Orai1 (A.1 and A.2) or the mutated CFP–Orai1(R91W) (A.3). Cell fluorescence was monitored both under resting conditions and upon stimulating for 1 min with 1 μM of TG. The histogram represents the means±s.e.m. of the colocalization index (R-value) acquired in several cells from several independent cell transfection experiments, as indicated. **P*<0.05 (Student's *t*-test). (B) NG115-401L cells were transfected either with YFP–STIM1-WT or YFP–STIM1-Y316F, and were additionally transfected with GFP–Orai1. Cells were stimulated for 1 min at 37°C with TG (200 nM) and then lysed. Cell lysates were immunoprecipitated (IP) with anti-STIM1 antibody and the immunoprecipitated proteins were subjected to SDS-PAGE (10% gels) and subsequent western blotting (WB) using anti-Orai1 antibody following the protocol described in the Materials and Methods. Membranes were re-probed with anti-STIM1 antibody as a protein loading control. Images and blots are representative of four to six independent cell transfections. Scale bars: 10 μm.

Journal of Cell Science (2019) 132, jcs226019. doi:10.1242/jcs.226019

immunoprecipitates of resting cells and this interaction was enhanced after store depletion. In contrast, the expression of the STIM1 Y316F mutant significantly reduced the interaction by 70% between both proteins upon cell stimulation with TG (Fig. 3B, right two lanes; $P<0.05$; $n=4$). Taken together, these findings suggest that phosphorylation of STIM1 at $Y^{316}$ is required for the association with Orai1, as previously suggested in human platelets (López et al., 2012). This mechanism might underlie the role of STIM1 $Y^{316}$ phosphorylation in the activation of $I_{CRAC}$ and SOCE.

### Phosphorylation of STIM1 $Y^{316}$ does not contribute to the conformational change of STIM1 during SOCE activation

It has been reported that $Ca^{2+}$ store depletion leads to a conformational change of STIM1 from a resting close state to a fully extended conformation, required for the interaction with and activation of Orai1, as demonstrated by using double-labeled YFP–STIM1–233-474–CFP (YFP–OASF–CFP; OASF, Orai1-activating small fragment) as a sensor of the intramolecular transition that leads to an extended conformation when binding to Orai1 (Muik et al., 2011). We explored whether STIM1 phosphorylation at $Y^{316}$ is relevant for the conformational change in HEK293 cells co-expressing Orai1 and either YFP–OASF–CFP or the YFP–OASF-Y316F–CFP mutant, following a previously reported procedure (Muik et al., 2011). As depicted in Fig. 4A, FRET analysis revealed no changes in the YFP fluorescence for either in resting cells or cells where $Ca^{2+}$ store depletion was induced by treatment with 2 µM TG. Considering that OASF may directly interact with Orai1 in the absence of stimuli, we repeated the experiments using a longer fragment of STIM1 known

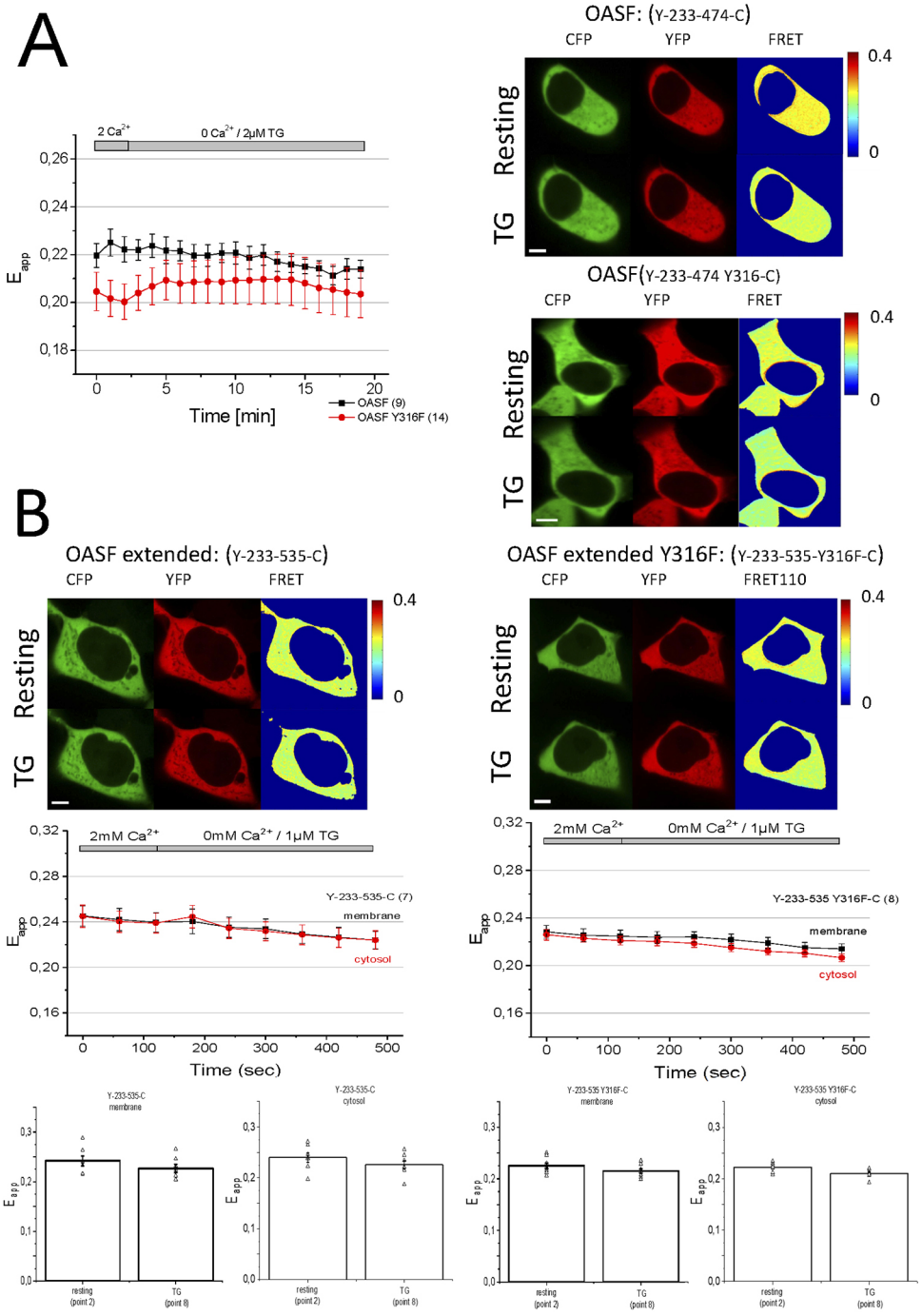


**Fig. 4. A structural conformation change in STIM1 is not driven by its phosphorylation at $Y^{316}$ residue.** (A,B) FRET analysis was performed in cells expressing either WT-OASF (233–474) (A, $n$=8–14 cells belonging to three independent experiments) or WT-OASF extended (233–535) (B, 2–8 cells belonging to three independent experiments) and with Y316F-OASF or Y316F-OASF extended, respectively. Upon confirming positive expression of the construct (CFP and YFP images), time-lapse experiments were performed, in which FRET derived from the CFP/YFP linked to the STIM1 fragments was estimated while SOCE was driven by using TG (1 to 2 µM in a $Ca^{2+}$-free medium, as indicated by the boxes above graphs) (graphs of $E_{app}$; mean±s.d.). Representative images are shown with the FRET indicated in pseudocolor according to the scale on the right. (A) FRET for cells transfected with OASF and Y316F-OASF. (B) FRET experiments of cells transfected with OASF extended (233–535). A re-evaluation of the FRET images looking for possible differences between the fluorescence recorded either within small portions of the cytosol (called points) or in portions located in close proximity to the plasma membrane, was performed as depicted in the histograms. Statistical analysis provided a $P<0.05$ (Student's $t$-test). Scale bars: 10 µm.

Journal of Cell Science (2019) 132, jcs226019. doi:10.1242/jcs.226019

as OASF extended (amino acids 233–535), which has been found to lack the ability to induce constitutive CRAC currents in the absence of stimuli (Muik et al., 2009). Similar to the observations when expressing OASF, no FRET changes were detected upon stimulation with TG (Fig. 4B). Furthermore, no differences in FRET were detected either in the cytosol or near the plasma membrane, where Orai1 is located (Fig. 4B, bar graphs). These findings indicate that $Y^{316}$ phosphorylation in itself does not induce the intramolecular transition into an extended conformation.

### STIM1 $Y^{316}$ phosphorylation might facilitate its interaction with SARAF

We further evaluated whether STIM1 phosphorylation at $Y^{316}$ is important for the interaction with STIM1 regulatory proteins. SARAF has emerged as a physiological inhibitor of STIM1 (Palty et al., 2012) and interacts with the CTID region of STIM1. It has been reported that the four conserved glutamate residues ($E^{318}$–$E^{322}$) of the auto-inhibitory domain of CC1 interact with the STIM1 (448–490) lobe of the CTID (Jha et al., 2013). Interestingly, in cells with a low expression of STIM1, like NG115-401L cells, SARAF interacts with and activates Orai1 (Albarran et al., 2016; Palty et al., 2012). Considering that $Y^{316}$ is very close to the four glutamate residues in CC1, we explored whether phosphorylation of STIM1 at $Y^{316}$ is relevant for SARAF–STIM1 interaction by assessing co-immunoprecipitation between SARAF and STIM1 in NG115-401L cells expressing STIM1 WT or the STIM1 Y316F mutant. As shown in Fig. 5, and as previously reported (Albarran et al., 2016), treatment with TG for 1 min did not significantly modify the interaction between SARAF and STIM1-WT as compared to that seen in resting cells. Interestingly, impairment of STIM1 phosphorylation at $Y^{316}$ by expression of the STIM1 Y316F mutant significantly increased the TG-induced SARAF–STIM1 interaction by 38% (see Fig. 5A lane 4 versus lane 2; $n$=4; $P$<0.05). These results strongly indicate that phosphorylation of STIM1 at $Y^{316}$ is required for the dissociation from SARAF, and thus, impairment of STIM1 phosphorylation at $Y^{316}$ might lead to an enhanced association with SARAF, which, in turn, would restrict the interaction of STIM1 with Orai1 attenuating SOCE and $I_{CRAC}$.

To further explore this possibility, we analyzed TG-induced $Ca^{2+}$ influx in NG115-401L cells transfected either with STIM1 WT or the STIM1 Y316F mutant, as well as plasmids expressing shRNA targeting SARAF (shSARAF) or scramble shRNA. As depicted in Fig. 6A, and as expected, in NG115-401L cells overexpressing STIM1 WT reconstitutes SOCE. The increase in SOCE is revealed by analyzing the area under the curves (see histogram in Fig. 6), and the $K_1$ of the $Ca^{2+}$ traces ($3.4\times10^{-5}\pm1.3\times10^{-6}$ versus $6.8\times10^{-5}\pm2.5\times10^{-6}$ in cells transfected with the empty vector or with the STIM1 WT). Co-transfection of STIM1 WT together with shSARAF resulted in a

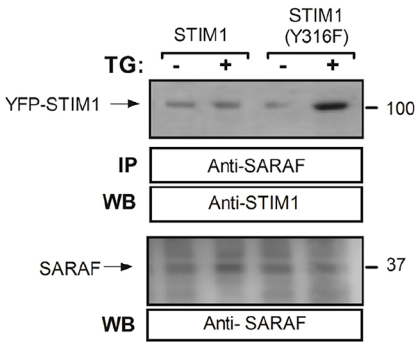


**Fig. 5. Impairment of STIM1 phosphorylation at $Y^{316}$ favors its interaction with SARAF.** NG115-401L cells were transfected either with YFP–STIM1-WT or YFP–STIM1-Y316F. Cells were stimulated for 1 min at 37°C with TG (1 µM) and lysed. Whole-cell lysates were immunoprecipitated (IP) with anti-SARAF antibody and the resulting precipitated proteins were analyzed by western blotting (WB) using an anti-STIM1 antibody as described in the Materials and Methods. Membranes were re-probed with anti-SARAF antibody as a protein loading control. Blots are representative of four to six independent cell transfections.

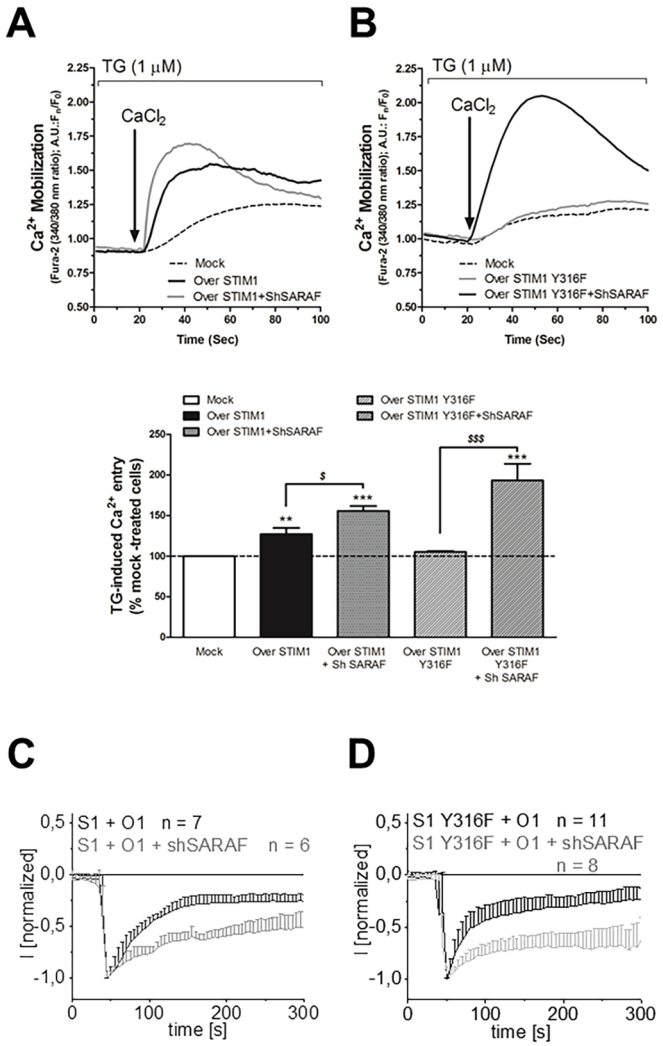


**Fig. 6. SARAF expression silencing reverses the inhibitory role of the STIM1 Y316F mutant in SOCE.** NG115-401L cells were transfected either with STIM1 WT (A) or the STIM1 Y316F mutant (B) (i.e. overexpression, denoted by over) in the absence or presence of the shSARAF. After 48 h, cells were loaded with fura-2 and suspended in a $Ca^{2+}$-free medium (EGTA, 75 µM was added) and then stimulated with TG (1 µM) followed by re-addition of 300 µM $CaCl_2$ for 4 min to detect SOCE. Traces are representative of six independent experiments including 10–20 cells. The bar graph represents $Ca^{2+}$ entry in the different conditions expressed as mean±s.e.m. $^{**}P$<0.01, $^{***}P$<0.001 as compared to mock-treated cells; $^{\$}P$<0.05, $^{\$\$\$}P$<0.001 as compared to cells not transfected with shSARAF (ANOVA, Dunnett's test was used for comparing all experimental conditions with Mock cells; Student's $t$-test was used for comparing among cells where SARAF was silenced with respect to the same experimental condition and expressing native SARAF). (C,D) HEK293 cells were co-transfected with Orai1 (O1) and either STIM1 WT (S1; C) or STIM1 Y316F (S1 Y316F; D), and shSARAF or scrambled plasmid. SCDI was estimated as described in the Materials and Methods. Data are presented as the mean±s.d. of normalized currents from 6 to 11 cells are presented as a time course for 5 min upon inward current activation, as indicated.

Journal of Cell Science (2019) 132, jcs226019. doi:10.1242/jcs.226019

further increase in SOCE ($K_1$, $8.8\times10^{-5}\pm1.7\times10^{-6}$), which reveals the inhibitory role of SARAF previously reported (Albarran et al., 2016, Palty et al., 2012).

Expression of the STIM1 Y316F mutant in NG115-401L cells marginally reconstitutes SOCE in these cells, as shown above (Fig. 6B and Fig. 2). Interestingly, SARAF knockdown using shRNA technology in cells expressing the STIM1 Y316F mutant leads to a significant increase in SOCE, thus indicating that SARAF is involved in the inhibition of SOCE observed in cells expressing the STIM1 Y316F mutant (Fig. 6B). SOCE in cells transfected with shSARAF was found to be significantly greater in cells expressing the STIM1 Y316F mutant than in cells expressing STIM1 WT (Fig. 6B and bar graph), which indicates that, in addition to the role of STIM1 phosphorylation at $Y^{316}$ in the regulation of the STIM1–SARAF interaction, this posttranslational modification might regulate other SARAF-independent processes. Finally, we explored the effect of the STIM1 Y316F mutation in SCDI, which has been reported to be regulated by SARAF. As depicted in Fig. 6C,D, we performed patch-clamp experiments in HEK293 cells according to experimental conditions previously described (Jha et al., 2013). A greater SCDI was observed in cells transfected with the STIM1 Y316F and Orai1 as compared with cells expressing STIM1 WT and Orai1 (Fig. 6C,D, black traces), which is consistent with the greater SARAF–STIM1-Y316F interaction reported above (Fig. 5). These data are also consistent with the inhibition in SOCE and $I_{CRAC}$ found in cells transfected with STIM1 Y316F (Fig. 2). As shown in Fig. 6C,D, SARAF knockdown attenuated SCDI in cells transfected with STIM1 WT and the STIM1 Y316F mutant, leading to a similar inactivation in both experimental conditions, and thus indicating that the greater SCDI induced by transfection of the STIM1 mutant is dependent on SARAF.

## DISCUSSION

There is a growing body of evidence supporting a role for STIM1 phosphorylation in the regulation of SOCE. Although most studies have been focused on phosphorylation of STIM1 at serine or threonine residues, a recent study has revealed that Pyk-2-dependent phosphorylation of STIM1 at $Y^{361}$ plays an essential role in the recruitment of Orai1 into STIM1 puncta during the activation of SOCE in endothelial cells, which has been associated with an increase in endothelial barrier permeability (Yazbeck et al., 2017). Although in the aforementioned study the authors presented evidenced against $Y^{316}$ as the target residue of kinases in favor of $Y^{361}$; Yu and coworkers envisaged that the $Y^{316}$ residue plays a relevant role in maintaining STIM1 in a quiescent state in resting cells, as the expression of the STIM1 Y316A mutant in itself resulted in STIM1 oligomerization. The auto-inhibitory role of STIM $Y^{316}$ has been attributed to either the intramolecular interaction of the $Y^{316}$ with the SOAR domain, through hydrogen and/or hydrophobic bonds, or an intermolecular interaction mediated through repulsive forces, which would maintain STIM1 in a quiescent state (Yu et al., 2013). Here, we provide evidence for a role of phosphorylation of STIM1 at $Y^{316}$ in the STIM1 and Orai1 colocalization at ER–PM junctions as well as for the activation of $I_{CRAC}$ and SOCE. Furthermore, we described for the first time that phosphorylation of STIM1 at $Y^{316}$ modulates the interaction between STIM1 and its regulator SARAF. SARAF has been reported to interact with STIM1 in a dynamic manner. According to this model SARAF is associated with STIM1 in resting cells but, upon $Ca^{2+}$ store depletion, SARAF dissociates from STIM1, allowing STIM1 oligomerization and interaction with Orai1 channels in the PM, followed by re-interaction with STIM1 to activate slow $Ca^{2+}$-dependent inactivation of Orai1 (Albarran et al., 2016; Jha et al., 2013; Palty et al., 2012). The role of the phosphorylation of STIM1 at $Y^{316}$ in the interaction between STIM1 and SARAF might provide a molecular basis for the findings reported by Yu and coworkers (Yu et al., 2013). Discrepancies in the tyrosine residue that is or could be phosphorylated in STIM1 might be indicative of the presence of different STIM1 regulatory pathways that would involve different tyrosine kinases, or perhaps, could indicate that these kinases are also sequentially activated. In fact, a recent study reported that SOCE activation by STIM1 is required for Pyk-2 activation in human lung microvascular endothelial cells, which then resulted in Pyk-2-dependent Src family protein activation (Soni et al., 2017). In platelets, we have reported that $pp60^{Src}$ (Src itself) interacts with and phosphorylates STIM1, which requires changes in the $[Ca^{2+}]_c$, thus regulating SOCE (López et al., 2012). In addition, STIM1 phosphorylation by Btk in platelets does not require changes in $[Ca^{2+}]_c$. Hence, Pyk-2-mediated STIM1 phosphorylation might contribute to the regulation of STIM1 function due to the phosphorylation of $Y^{361}$, which might require $p60^{Src}$ activation, while $Y^{316}$ would be targeted by Btk. Nonetheless, future investigation will be required in order to confirm this hypothesis.

In addition, previous proximity ligation assay and co-immunoprecipitation studies, have shown that there is detectable interaction between SARAF and STIM1 under resting conditions that is significantly reduced after $Ca^{2+}$ store depletion using TG, reaching a minimum 30 s after stimulation and then this interaction increased, and exceeding the resting level between ∼60 and ∼120 s after stimulation (Albarran et al., 2016). Here, we show that 60 s after stimulation with TG the interaction between SARAF and STIM1 is significantly greater in cells expressing the STIM1 Y316F mutant, which indicates that phosphorylation of STIM1 at $Y^{316}$ plays a negative role in the association of STIM1 with its negative regulator SARAF. Based on previous findings (Albarran et al., 2016; Jha et al., 2013; Palty et al., 2012) and our observations (see Fig. 6), the enhanced association of SARAF with STIM1 might explain the attenuation in SOCE and $I_{CRAC}$, and the colocalization of STIM1 with Orai1 observed in cells expressing the STIM1 Y316F mutant as compared to what is seen in cells expressing STIM1 WT.

The reduction in $I_{CRAC}$ and SOCE observed in cells with impaired phosphorylation at $Y^{316}$ cannot be attributed to inhibition of STIM1 puncta formation, as evidenced by confocal microscopy (see Fig. 3) and previously reported (Yu et al., 2013). This effect is more likely to occur through attenuation of the association between STIM1 and Orai1 (as shown in Fig. 3) that induced by the association of STIM1 with SARAF. Hence, here, we present for the first time, evidence that phosphorylation at $Y^{316}$ might finetune the formation of the CRAC signaling complex, which would contribute to dissociation of SARAF from STIM1 and regulation of SCDI, as depicted in Fig. 7. In addition, our results indicate that mutation of the tyrosine residue into phenylalanine is an efficient mechanism to analyze STIM1 phosphorylation during SOCE, since this change might avoid the constitutive activation of STIM1 observed when $Y^{316}$ is replaced by alanine or aspartate residues, as previously shown (Yu et al., 2013).

A role for $Ca^{2+}$ store depletion-dependent tyrosine phosphorylation in the activation of SOCE has long been proposed in different cell types (López et al., 2012; Redondo et al., 2005; Rosado et al., 2000; Sargeant et al., 1993; Yu et al., 2013). The identification of two key residues ($Y^{316}$ and $Y^{361}$) that act to modulate STIM1 function, and subsequently, alter activation of $I_{CRAC}$ and SOCE, provides compelling evidence for a relevant role of tyrosine phosphorylation in the regulation of $Ca^{2+}$ influx, which might represent a novel target for the study of the molecular basis of disease.

Journal of Cell Science (2019) 132, jcs226019. doi:10.1242/jcs.226019

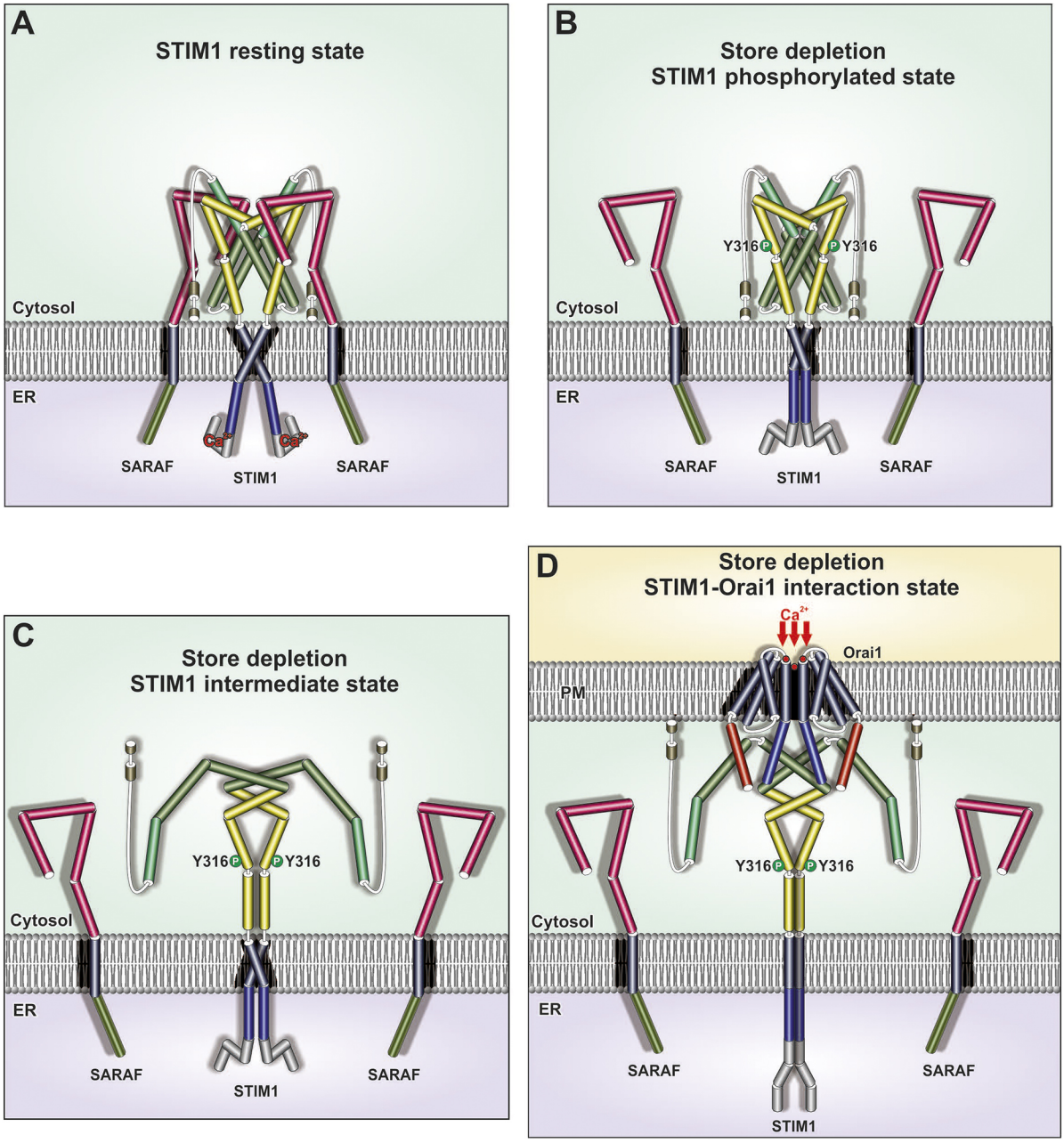


**Fig. 7. Schematic representation of the regulatory mechanism of STIM1 and Orai1 interaction by SARAF through tyrosine phosphorylation of STIM1 at the Y316 residue.** (A) STIM1 binds SARAF under resting conditions. (B) STIM1 Y316 phosphorylation would facilitate SARAF dissociation. (C) STIM1–SARAF dissociation leads to the full extended conformation. (D) STIM1 interacts with and activates Orai1 allowing $Ca^{2+}$ entry.

## MATERIALS AND METHODS

### Materials

Lipofectamine® was from Thermo Fisher Scientific, transfectin was from Bio-Rad, kit C for AMAXA® was provided by Lonza. Fura 2/AM, mouse anti-phosphotyrosine (4G10) antibody (cat. no. 05-321), rabbit polyclonal anti-SARAF (TMEM66) antibody (epitope amino acids 33–62 of the N-terminal region of human TMEM66; cat. no. PA5-24237) and mouse monoclonal anti-STIM1 antibody (clone 44 GOK$^{-1}$, epitope: amino acids 25–139 of human STIM1; cat. no. 610954) were supplied by Merck Millipore. Horseradish peroxidase (HRP)-conjugated secondary antibodies were ordered from Jackson ImmunoResearch laboratories. TG and anti-Orai1 (C-terminal; cat. no. SAB4200273) antibody as well as other reagents used, of analytical grade, were provided by Sigma-Aldrich.

### Cell types and transfection

MEG-01, HEK293 and NG115-401L (NG115) cells were purchased from the ATCC, and cultured following the manufacturer's recommendations. NG115-401L and HEK293 cells were transfected using Lipofectamine, while MEG-01 cell transfection was performed using kit C for the AMAXA nucleofector device. Human STIM1 (accession number NM_003156) N-terminally tagged with EYFP was kindly provided by the Meyer's laboratory, Stanford University, Stanford, CA. For double-tagged STIM1 constructs, CFP was cloned into pEYFP-C2 via the SacII and XbaI sites, and the OASF STIM1 fragment (233–474) and OASF extended STIM1 fragment (233–535) were introduced via the EcoRI and SacII sites. Point mutations (Y316F and Y361F) were generated by using the QuikChange XL site-directed mutagenesis kit (Stratagene). The integrity of all resulting clones was confirmed by sequence analysis (Eurofins). Following transfection

protocols, the percentage of transfected cells was confirmed by visualizing the YFP emission under a fluorescence microscopy. In addition, we used shSARAF generated by our research group (Albarran et al., 2016) in order to reduce SARAF expression in NG115-401L cells as previously described.

### Cell stimulation, protein isolation and western blotting

Cells were suspended in HEPES-buffered saline (HBS; containing in mM: 145 NaCl, 10 HEPES pH 7.40, 10 D-glucose, 5 KCl, 1 $Mg_2SO_4$) and supplemented with 50 µM $CaCl_2$. Cells were stimulated with 200 nM TG in a $Ca^{2+}$-free HBS (75 µM of EGTA added) and then lysed using NP40 buffer (containing in mM: 20 Tris-HCl pH 8.0, 1.37 NaCl, 2 EDTA, 10% glycerol and 1% nodidet P-40) and supplemented with a protease cocktail (Roche) and $Na_3VO_4$. Cell lysates were immunoprecipitated with anti-STIM1 (2 µM) or anti-SARAF (TMEM66) antibody (2 µM). Immunoprecipitated proteins were separated by 10% SDS-PAGE and subsequently transferred onto a nitrocellulose membrane. Membranes were probed with anti-phosphotyrosine (4G10) antibody for 1 h at room temperature, anti-Orai1 antibody overnight 4°C and anti-SARAF antibody for 1 h at room temperature (these antibodies were diluted in Tris-buffered saline with 0.1% Tween 20 at 1:1000, 1:250 and 1:1000, respectively). Upon membranes being exposed to enhanced chemiluminescence reagent for 4 min, blot densitometry was estimated using the C-digit chemiluminescent western blot scanner (Licor). Data were normalized to the amount of protein recovered by the antibody used for the immunoprecipitation.

### Measurement of $[Ca^{2+}]_c$

Scramble- and STIM1-transfected cells were loaded with fura 2 by incubation with 2 µM fura 2-AM for 30 min at room temperature. Cells were then suspended in HBS containing 50 µM $CaCl_2$. Coverslips were placed in a perfusion chamber of an inverted microscope and excited alternatively at 340 and 380 nm. Fura 2 fluorescence was detected at 515 nm using a cooled digital CCD camera (Hisca CCD C-6790, Hamamatsu, Japan) and recorded using Aquacosmos 2.5 software (Hamamatsu Photonics, Hamamatsu, Japan). Resulting traces were normalized to the fluorescence emitted by the cells under resting conditions ($F_n/F_0$). SOCE was measured by determining the integral of the rise in $[Ca^{2+}]_c$ for 1.5–2 min after the addition of 0.3–1 mM $CaCl_2$ to TG-treated cells (0.2–1 µM), taking a sample every second, and is expressed as nM s (López et al., 2005). Additionally, we determined the $K_1$ the constant of the two-phase exponential decay equation [$y=A(1-e^{-K1t})e^{-K2t}$], which represents the exponential increase constant of the $Ca^{2+}$ rise during SOCE activation (López et al., 2005).

### Intracellular colocalization of STIM1 and Orai1 determination

HEK293 cells were co-transfected with CFP–Orai1 and either YFP–STIM1-WT or YFP–STIM1-Y316F plasmids. An additional set of experiments were performed using a CFP–Orai1(R91W) overexpression plasmid, which was considered as an internal experimental control, evidencing that puntual modification of the proteins do not necessarily involve changes in their interaction pattern. Cells were observed under the confocal microscope in either the resting condition or upon stimulation with TG (1 µM) for 1 min. Fluorescence of both YFP and CFP were recorded in order to analyze protein localization as evidenced by merge images.

### Platch-clamp experiments

Electrophysiological experiments were performed at 20–24°C after 12–48 h of cell transfection with transfectin (Bio-Rad) and 1 µg of the Orai1 and STIM1-WT or STIM1-Y316F constructs. We used the patch-clamp technique in the whole-cell recording configuration for current measurements, with voltage ramps applied every 5 s from a holding potential of 0 mV, covering a range of −90 to +90 mV over 1 s. The internal pipette solution for passive store depletion contained (in mM): 3.5 $MgCl_2$, 145 cesium methanesulfonate, 8 NaCl, 10 HEPES pH 7.4, 20 EGTA, pH 7.2. Extracellular solution consisted of (in mM): 145 NaCl, 5 CsCl, 1 $MgCl_2$, 10 HEPES, 10 glucose, 10 $CaCl_2$. To measure SCDI, the pipette solution contained (in mM, adjusted to pH 7.2): 3.5 $MgCl_2$, 145 cesium methanesulfonate, 8 NaCl, 10 HEPES, 1,2 EGTA. After establishing the whole-cell configuration, the cells were kept in a $Ca^{2+}$-free solution [(in mM): 140 NaCl, 5 KCl, 1 MgCl, 10 HEPES and 10 glucose] for 5 min to allow store depletion before exposing the cells to the extracellular solution containing 10 mM $Ca^{2+}$ (Jha et al., 2013). All currents were leak corrected by subtracting either the value from the initial voltage ramps obtained shortly after break-in with no visible current activation or the remaining currents after 10 mM $La^{3+}$ application at the end of the experiment, with both yielding identical results.

### Confocal microscopy

Confocal Förster resonance energy transfer microscopy (FRET) was performed on HEK293 cells, as previously described (Derler et al., 2006). In brief, for recording fluorescence images we used a QLC100 Real-Time Confocal System (VisiTech Int.) connected to two Photometrics CoolSNAPHQ monochrome cameras (Roper Scientific) and a dual port adapter (dichroic: 505lp; cyan emission filter: 485-30; yellow emission filter: 535-50; Chroma Technology Corp.). This system was implemented with an Axiovert 200M microscope (Zeiss, Germany) in conjunction with two diode lasers (445 nm and 515 nm) (Visitron Systems). Visiview 2.1.1 software (Visitron Systems) was used for image acquisition and controlling the confocal system. As required, we performed an image correction, to modulate for cross-talk and cross-excitation, before to the calculation; appropriate cross-talk calibration factors were determined for each construct on the raw data from the FRET experiments. After threshold determination and background subtraction, the corrected FRET ($E_{app}$) was calculated on a pixel-to-pixel basis with custom-made software (Zal and Gascoigne, 2004) integrated in MatLab 7.0.4 according to the method published previously (Singh et al., 2006), with a microscope-specific constant G value of 2.0. All experiments were performed at room temperature.

### Statistical analysis

Analysis of statistical significance was performed with a unpaired Student's *t*-test or one-way analysis of variance (ANOVA) combined with the Dunnett's test. The Pearson correlation coefficient (R-value) was used to measure the strength of the linear association/colocalization between STIM1 and Orai1 variants. Overall, only values with $P<0.05$ were accepted as significant throughout the present research.

#### Acknowledgements

We are grateful to Dr A. Quesada and Prof. X. Pingyong (University of Extremadura and Institute of Biophysic and Chinese Academy of Sciences, respectively) for their technical support. Furthermore, we like also thank to Dr T. Meyer for providing the YFP-STIM1 overexpression plasmid.

#### Competing interests

The authors declare no competing or financial interests.

#### Author contributions

E.L., I.F., I.J., C.C., I.D. and M.M. have designed and performed the experiments. G.M.S., T.S., J.A.R. and P.C.R. have designed, discussed and drafted the manuscript.

#### Author contributions

Conceptualization: I.F., I.J., M.M., J.A.R., P.C.R.; Methodology: E.L., I.F., I.J., I.D., M.M., C.C., P.C.R.; Software: I.F., I.D., P.C.R.; Validation: M.M., G.M.S., T.S.; Formal analysis: I.F., P.C.R.; Investigation: I.F., I.D., M.M., C.C., P.C.R.; Data curation: E.L., I.J., I.D., M.M., C.C., J.A.R., P.C.R.; Writing - original draft: I.F., J.A.R., P.C.R.; Writing - review & editing: G.M.S., T.S., J.A.R., P.C.R.; Supervision: G.M.S., T.S., P.C.R.; Project administration: J.A.R.; Funding acquisition: T.S., J.A.R., P.C.R.

#### Funding

This work was supported by the Ministerio de Economía y Competitividad (MINECO; BFU2013-45564C2-1-P and BFU2016-74932-C2) and Consejería de Educación y Empleo, Junta de Extremadura -FEDER (GR18061 and IB16046). E.L. and I.J. have been benefited from a contract of the Instituto de Salud Carlos III (ISCIII) (FI10/00573) and MINECO. C.C. had a predoctoral fellowship of the Junta de Extremadura. I.F. is funded by the Austrian Science Fund (FWF), grant number P28872.

#### Supplementary information

Supplementary information available online at http://jcs.biologists.org/lookup/doi/10.1242/jcs.226019.supplemental

## References


**Albarran, L., Lopez, J. J., Amor, N. B., Martin-Cano, F. E., Berna-Erro, A., Smani, T., Salido, G. M. and Rosado, J. A.** (2016). Dynamic interaction of SARAF with STIM1 and Orai1 to modulate store-operated calcium entry. *Sci. Rep.* **6**, 24452. doi:10.1038/srep24452

**Casas-Rua, V., Tomas-Martin, P., Lopez-Guerrero, A. M., Alvarez, I. S., Pozo-Guisado, E. and Martin-Romero, F. J.** (2015). STIM1 phosphorylation triggered by epidermal growth factor mediates cell migration. *Biochim. Biophys. Acta* **1853**, 233-243. doi:10.1016/j.bbamcr.2014.10.027

**Derler, I., Hofbauer, M., Kahr, H., Fritsch, R., Muik, M., Kepplinger, K., Hack, M. E., Moritz, S., Schindl, R., Groschner, K. et al.** (2006). Dynamic but not constitutive association of calmodulin with rat TRPV6 channels enables fine tuning of $Ca^{2+}$-dependent inactivation. *J. Physiol.* **577**, 31-44. doi:10.1113/jphysiol.2006.118661

**Derler, I., Jardin, I. and Romanin, C.** (2016). Molecular mechanisms of STIM/Orai communication. *Am. J. Physiol. Cell Physiol.* **310**, C643-C662. doi:10.1152/ajpcell.00007.2016

**Fahrner, M., Muik, M., Schindl, R., Butorac, C., Stathopulos, P., Zheng, L., Jardin, I., Ikura, M. and Romanin, C.** (2014). A coiled-coil clamp controls both conformation and clustering of stromal interaction molecule 1 (STIM1). *J. Biol. Chem.* **289**, 33231-33244. doi:10.1074/jbc.M114.610022

**Fluckiger, A.-C., Li, Z., Kato, R. M., Wahl, M. I., Ochs, H. D., Longnecker, R., Kinet, J.-P., Witte, O. N., Scharenberg, A. M. and Rawlings, D. J.** (1998). Btk/Tec kinases regulate sustained increases in intracellular $Ca^{2+}$ following B-cell receptor activation. *EMBO J.* **17**, 1973-1985. doi:10.1093/emboj/17.7.1973

**Haniu, H., Komori, N., Takemori, N., Singh, A., Ash, J. D. and Matsumoto, H.** (2006). Proteomic trajectory mapping of biological transformation: Application to developmental mouse retina. *Proteomics* **6**, 3251-3261. doi:10.1002/pmic.200500813

**Hoda, J.-C., Zaghetto, F., Singh, A., Koschak, A. and Striessnig, J.** (2006). Effects of congenital stationary night blindness type 2 mutations R508Q and L1364H on Cav1.4 L-type $Ca^{2+}$ channel function and expression. *J. Neurochem.* **96**, 1648-1658. doi:10.1111/j.1471-4159.2006.03678.x

**Jha, A., Ahuja, M., Maléth, J., Moreno, C. M., Yuan, J. P., Kim, M. S. and Muallem, S.** (2013). The STIM1 CTID domain determines access of SARAF to SOAR to regulate Orai1 channel function. *J. Cell Biol.* **202**, 71-79. doi:10.1083/jcb.201301148

**Korzeniowski, M. K., Manjarres, I. M., Varnai, P. and Balla, T.** (2010). Activation of STIM1-Orai1 involves an intramolecular switching mechanism. *Sci. Signal.* **3**, ra82. doi:10.1126/scisignal.2001122

**Lee, K. P., Yuan, J. P., Hong, J. H., So, I., Worley, P. F. and Muallem, S.** (2010). An endoplasmic reticulum/plasma membrane junction: STIM1/Orai1/TRPCs. *FEBS Lett.* **584**, 2022-2027. doi:10.1016/j.febslet.2009.11.078

**Lee, H.-J., Bae, G.-U., Leem, Y.-E., Choi, H.-K., Kang, T. M., Cho, H., Kim, S.-T. and Kang, J.-S.** (2012). Phosphorylation of Stim1 at serine 575 via netrin-2/Cdo-activated ERK1/2 is critical for the promyogenic function of Stim1. *Mol. Biol. Cell* **23**, 1376-1387. doi:10.1091/mbc.e11-07-0634

**Liao, Y., Erxleben, C., Abramowitz, J., Flockerzi, V., Zhu, M. X., Armstrong, D. L. and Birnbaumer, L.** (2008). Functional interactions among Orai1, TRPCs, and STIM1 suggest a STIM-regulated heteromeric Orai/TRPC model for SOCE/Icrac channels. *Proc. Natl. Acad. Sci. USA* **105**, 2895-2900. doi:10.1073/pnas.0712288105

**López, J. J., Camello-Almaraz, C., Pariente, J. A., Salido, G. M. and Rosado, J. A.** (2005). $Ca^{2+}$ accumulation into acidic organelles mediated by $Ca^{2+}$- and vacuolar H+-ATPases in human platelets. *Biochem. J.* **390**, 243-252. doi:10.1042/BJ20050168

**López, E., Jardin, I., Berna-Erro, A., Bermejo, N., Salido, G. M., Sage, S. O., Rosado, J. A. and Redondo, P. C.** (2012). STIM1 tyrosine-phosphorylation is required for STIM1-Orai1 association in human platelets. *Cell. Signal.* **24**, 1315-1322. doi:10.1016/j.cellsig.2012.02.012

**Ma, G., Wei, M., He, L., Liu, C., Wu, B., Zhang, S. L., Jing, J., Liang, X., Senes, A., Tan, P. et al.** (2015). Inside-out $Ca^{2+}$ signalling prompted by STIM1 conformational switch. *Nat. Commun.* **6**, 7826. doi:10.1038/ncomms8826

**Mills, R. D., Mita, M. and Walsh, M. P.** (2015). A role for the $Ca^{2+}$-dependent tyrosine kinase Pyk2 in tonic depolarization-induced vascular smooth muscle contraction. *J. Muscle Res. Cell Motil.* **36**, 479-489. doi:10.1007/s10974-015-9416-2

**Muik, M., Fahrner, M., Derler, I., Schindl, R., Bergsmann, J., Frischauf, I., Groschner, K. and Romanin, C.** (2009). A cytosolic homomerization and a modulatory domain within STIM1 C terminus determine coupling to ORAI1 channels. *J. Biol. Chem.* **284**, 8421-8426. doi:10.1074/jbc.C800229200

**Muik, M., Fahrner, M., Schindl, R., Stathopulos, P., Frischauf, I., Derler, I., Plenk, P., Lackner, B., Groschner, K., Ikura, M. et al.** (2011). STIM1 couples to ORAI1 via an intramolecular transition into an extended conformation. *EMBO J.* **30**, 1678-1689. doi:10.1038/emboj.2011.79

**Palty, R., Raveh, A., Kaminsky, I., Meller, R. and Reuveny, E.** (2012). SARAF inactivates the store operated calcium entry machinery to prevent excess calcium refilling. *Cell* **149**, 425-438. doi:10.1016/j.cell.2012.01.055

**Perni, S., Dynes, J. L., Yeromin, A. V., Cahalan, M. D. and Franzini-Armstrong, C.** (2015). Nanoscale patterning of STIM1 and Orai1 during store-operated $Ca^{2+}$ entry. *Proc. Natl. Acad. Sci. USA* **112**, E5533-E5542. doi:10.1073/pnas.1515606112

**Pozo-Guisado, E., Campbell, D. G., Deak, M., Alvarez-Barrientos, A., Morrice, N. A., Alvarez, I. S., Alessi, D. R. and Martin-Romero, F. J.** (2010). Phosphorylation of STIM1 at ERK1/2 target sites modulates store-operated calcium entry. *J. Cell Sci.* **123**, 3084-3093. doi:10.1242/jcs.067215

**Pozo-Guisado, E., Casas-Rua, V., Tomas-Martin, P., Lopez-Guerrero, A. M., Alvarez-Barrientos, A. and Martin-Romero, F. J.** (2013). Phosphorylation of STIM1 at ERK1/2 target sites regulates interaction with the microtubule plus-end binding protein EB1. *J. Cell Sci.* **126**, 3170-3180. doi:10.1242/jcs.125054

**Redondo, P. C., Ben-Amor, N., Salido, G. M., Bartegi, A., Pariente, J. A. and Rosado, J. A.** (2005). $Ca^{2+}$-independent activation of Bruton's tyrosine kinase is required for store-mediated $Ca^{2+}$ entry in human platelets. *Cell. Signal.* **17**, 1011-1021. doi:10.1016/j.cellsig.2004.11.019

**Rosado, J. A., Graves, D. and Sage, S. O.** (2000). Tyrosine kinases activate store-mediated $Ca^{2+}$ entry in human platelets through the reorganization of the actin cytoskeleton. *Biochem. J.* **351**, 429-437. doi:10.1042/bj3510429

**Sage, S. O., Sargeant, P., Merritt, J. E., Mahaut-Smith, M. P. and Rink, T. J.** (1992). Agonist-evoked $Ca^{2+}$ entry in human platelets. *Biochem. J.* **285**, 341-344. doi:10.1042/bj2850341

**Sargeant, P., Farndale, R. W. and Sage, S. O.** (1993). ADP- and thapsigargin-evoked $Ca^{2+}$ entry and protein-tyrosine phosphorylation are inhibited by the tyrosine kinase inhibitors genistein and methyl-2,5-dihydroxycinnamate in fura-2-loaded human platelets. *J. Biol. Chem.* **268**, 18151-18156.

**Sargeant, P., Farndale, R. W. and Sage, S. O.** (1994). Calcium store depletion in dimethyl BAPTA-loaded human platelets increases protein tyrosine phosphorylation in the absence of a rise in cytosolic calcium. *Exp. Physiol.* **79**, 269-272. doi:10.1113/expphysiol.1994.sp003762

**Sheridan, J. T., Gilmore, R. C., Watson, M. J., Archer, C. B. and Tarran, R.** (2013). 17beta-Estradiol inhibits phosphorylation of stromal interaction molecule 1 (STIM1) protein: implication for store-operated calcium entry and chronic lung diseases. *J. Biol. Chem.* **288**, 33509-33518. doi:10.1074/jbc.M113.486662

**Singh, A., Hamedinger, D., Hoda, J.-C., Gebhart, M., Koschak, A., Romanin, C. and Striessnig, J.** (2006). C-terminal modulator controls $Ca^{2+}$-dependent gating of Ca(v)1.4 L-type $Ca^{2+}$ channels. *Nat. Neurosci.* **9**, 1108-1116. doi:10.1038/nn1751

**Smyth, J. T., Petranka, J. G., Boyles, R. R., DeHaven, W. I., Fukushima, M., Johnson, K. L., Williams, J. G. and Putney, J. W. Jr.** (2009). Phosphorylation of STIM1 underlies suppression of store-operated calcium entry during mitosis. *Nat. Cell Biol.* **11**, 1465-1472. doi:10.1038/ncb1995

**Soni, D., Regmi, S. C., Wang, D.-M., DebRoy, A., Zhao, Y.-Y., Vogel, S. M., Malik, A. B. and Tiruppathi, C.** (2017). Pyk2 phosphorylation of VE-PTP downstream of STIM1-induced $Ca^{2+}$ entry regulates disassembly of adherens junctions. *Am. J. Physiol. Lung Cell. Mol. Physiol.* **312**, L1003-L1017. doi:10.1152/ajplung.00008.2017

**Thompson, J. L. and Shuttleworth, T. J.** (2015). Anchoring protein AKAP79-mediated PKA phosphorylation of STIM1 determines selective activation of the ARC channel, a store-independent Orai channel. *J. Physiol.* **593**, 559-572. doi:10.1113/jphysiol.2014.284182

**Yazbeck, P., Tauseef, M., Kruse, K., Amin, M.-R., Sheikh, R., Feske, S., Komarova, Y. and Mehta, D.** (2017). STIM1 phosphorylation at Y361 recruits orai1 to STIM1 puncta and induces $Ca^{2+}$ entry. *Sci. Rep.* **7**, 42758. doi:10.1038/srep42758

**Yu, J., Zhang, H., Zhang, M., Deng, Y., Wang, H., Lu, J., Xu, T. and Xu, P.** (2013). An aromatic amino acid in the coiled-coil 1 domain plays a crucial role in the auto-inhibitory mechanism of STIM1. *Biochem. J.* **454**, 401-409. doi:10.1042/BJ20130292

**Yuan, J. P., Zeng, W., Dorwart, M. R., Choi, Y.-J., Worley, P. F. and Muallem, S.** (2009). SOAR and the polybasic STIM1 domains gate and regulate Orai channels. *Nat. Cell Biol.* **11**, 337-343. doi:10.1038/ncb1842

**Zal, T. and Gascoigne, N. R. J.** (2004). Photobleaching-corrected FRET efficiency imaging of live cells. *Biophys. J.* **86**, 3923-3939. doi:10.1529/biophysj.103.022087

**Zhang, C. and Thomas, D. W.** (2016). Stromal Interaction Molecule 1 rescues store-operated calcium entry and protects NG115-401L cells against cell death induced by endoplasmic reticulum and mitochondrial oxidative stress. *Neurochem. Int.* **97**, 137-145. doi:10.1016/j.neuint.2016.04.002

**Zhang, C., Bose, D. D. and Thomas, D. W.** (2015). Paradoxical effects of sarco/endoplasmic reticulum $Ca^{2+}$-ATPase (SERCA) activator gingerol on NG115-401L neuronal cells: failure to augment ER $Ca^{2+}$ uptake and protect against ER stress-induced cell death. *Eur. J. Pharmacol.* **762**, 165-173. doi:10.1016/j.ejphar.2015.05.055

**Zhou, Y., Srinivasan, P., Razavi, S., Seymour, S., Meraner, P., Gudlur, A., Stathopulos, P. B., Ikura, M., Rao, A. and Hogan, P. G.** (2013). Initial activation of STIM1, the regulator of store-operated calcium entry. *Nat. Struct. Mol. Biol.* **20**, 973-981. doi:10.1038/nsmb.2625

**Zuo, W.-L., Du, J.-Y., Huang, J.-H., Li, S., Zhang, G., Chen, S.-L., Ruan, Y.-C., Cheng, C. H. K. and Zhou, W.-L.** (2011). Tyrosine phosphorylation modulates store-operated calcium entry in cultured rat epididymal basal cells. *J. Cell. Physiol.* **226**, 1069-1073. doi:10.1002/jcp.22429

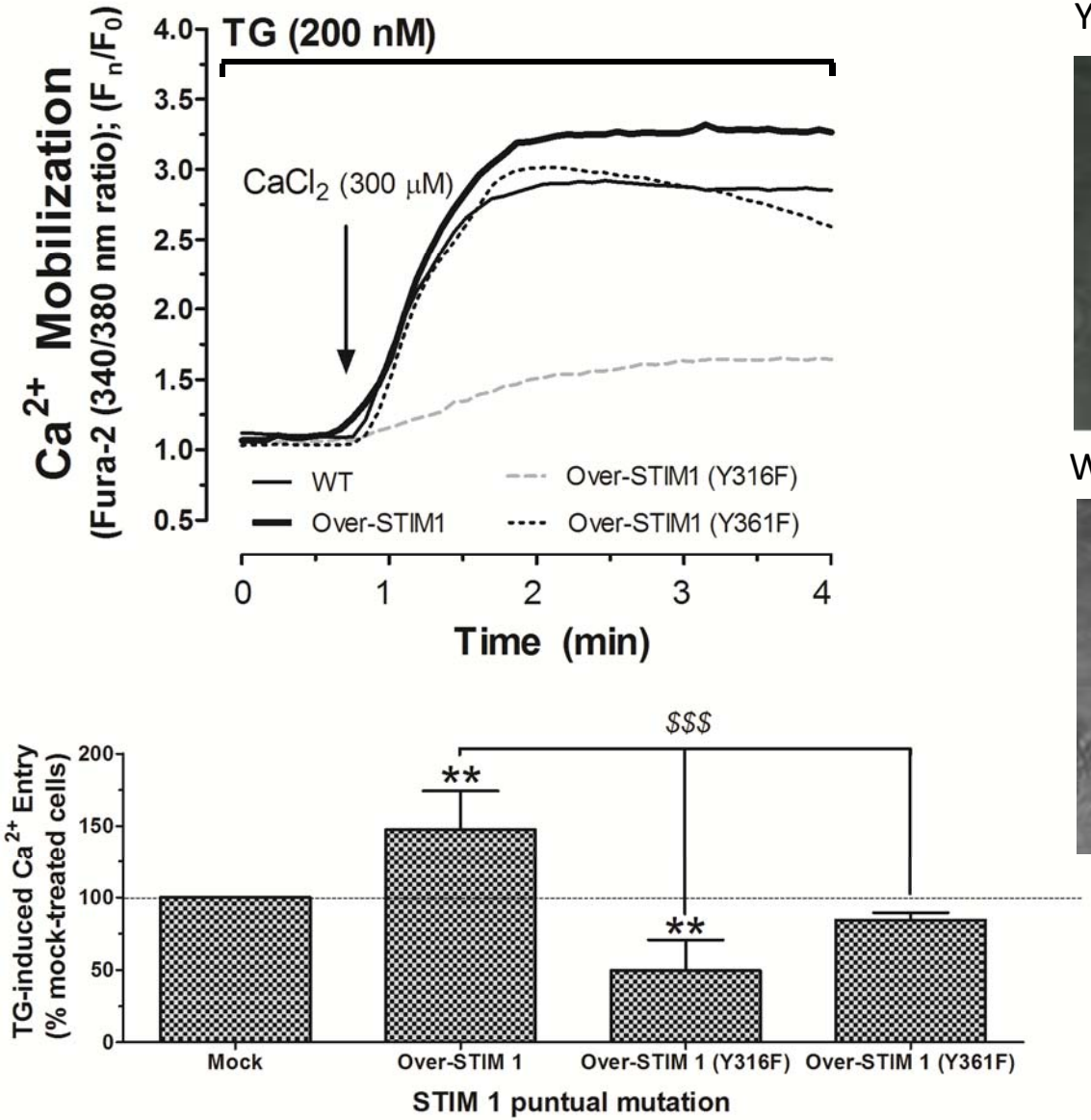


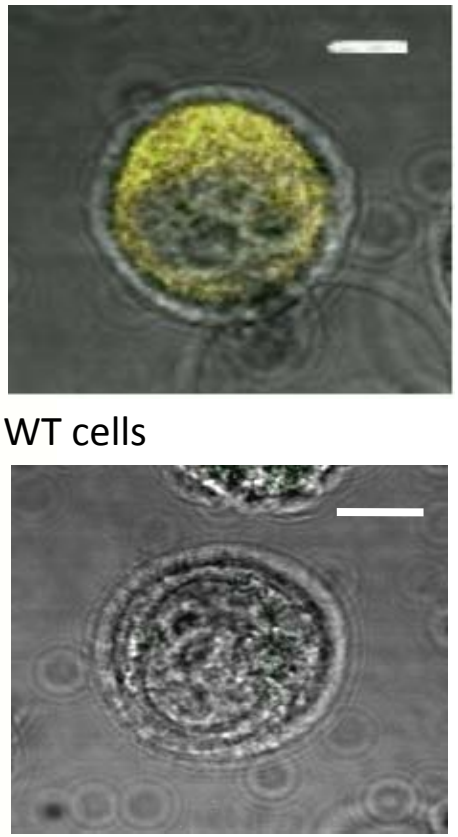


Figure S1. STIM1 Y316 tyrosine phosphorylation plays a relevant role in SOCE in MEG-01 cells. MEG-01 cells were transfected with the STIM1 WT or the indicated STIM1 mutants or empty vector (Mock). Upon being incubated with fura-2, cells were perfused with a $Ca^{2+}$-free medium (EGTA 75 μM was added) and then prestimulated with TG (200 nM). To detect SOCE $CaCl_2$ (300 μM) was added to the extracellular medium. Traces are representative of 4-6 independent cell transfections. Bar graph represents the differences in the TG-induced $Ca^{2+}$ entry estimated as described in Material and Methods section, and it is expressed as mean ± S.E.M.. ** represents $p < 0.01$ as compared to mock-treated cells. $^{\$\$\$}$ represents $p < 0.001$ as compared to cells expressing YFP-STIM1-WT. Images of MEG-01 cells positively expressing the YFP-STIM1 WT. Bar represents 50 μm.